Green Chemistry

Cite this: *Green Chem.*, 2012, **14**, 514

www.rsc.org/greenchem

PAPER

Carbon oxidation generated in diesel engines using iron-doped fuel

G. A. S. Schulz,[a] S. Tamborim,[b] G. Cardoso,[a] T. Santos,[a] E. Lissner[a] and R. Cataluña*[a]

Received 14th September 2011, Accepted 22nd November 2011
DOI: 10.1039/c2gc16147h

The soot oxidation activity of metallic iron nanoparticles was studied under real diesel engine conditions. Particulate matter (PM) was sampled at distinct temperatures, using fuels containing ferrocene. The results indicated an 80% reduction of accumulated PM using fuels doped with 50 ppm ferrocene at a temperature of 460 °C. Temperature-programmed catalytic oxidation tests indicated that PM oxidation in ferrocene-doped fuels starts at an approximately 200 °C lower temperature. The transmission electron microscopy (TEM) analysis of the PM revealed that soot agglomerates with and without the presence of Fe showed a similar morphology and that the average diameter of iron nanoparticles is 10 nm. The use of ferrocene-doped diesel fuels increases the speed of PM oxidation significantly, enabling the filter to self-regenerate at the average temperature of the exhaust gases. Moreover, 500 ppm of sulfur in fuels does not reduce the catalytic activity of iron nanoparticles in PM oxidation.

1. Introduction

The combustion process of diesel engines generates contaminants such as nitrogen oxides (NO_x), particulate matter (PM) and unburned hydrocarbons.[1] Today there is great interest in the improvement of technologies for controlling the emission of these pollutants due to the ever growing demand for automotive vehicles in large urban centers. The fundamental parameters for the development of diesel engines involve engine performance and emissions. Recently, the use of new electronic fuel injection systems and post-combustion treatment systems has been leading to satisfactory results in meeting current legislation.[2–7] However, meeting future regulations will require new developments for engines, fuels and catalytic systems.[7] Therefore, over the last few years, major investments have focused on improving engine/fuel/catalyst systems.

The organic fraction of PM (soot) is oxidized easily at a temperature of 600 °C.[8–12] Under normal operating conditions, the temperature of diesel engine exhaust gases is close to 450 °C, which is too low to begin the oxidation of soot. Thus, the technique of filter retention of PM followed by oxidation as the temperature rises through the injection of fuel into the exhaust gases has been one of the strategies employed commercially to meet PM emission limits. This strategy leads to a highly exothermic reaction that ends up damaging the filter element. A suitable solution to reduce the regeneration temperature of the filter element is the use of a catalyst to aid the oxidation of particulate matter. The greatest difficulty in catalyzing the oxidation reaction and reducing the reaction temperature is the contact between the catalyst and the soot particles. The use of catalysts with molten salts significantly increases the contact of the particles with the catalyst, reducing the onset temperature for oxidation from 600 to 400 °C.[13] The use of perovskite structures, microwave irradiation and the energy from the enthalpy of the oxidation reaction enable the formation of hot spots, with augmented speed of oxidation even at low exhaust gas temperatures.[14]

This work deals with the catalytic oxidation activity of nanostructures containing iron that are formed from the thermal decomposition of ferrocene. Carbon structures with elevated concentrations of iron are formed during diesel fuel vaporization in the combustion process. The oxidation activity was evaluated in reaction tests at a programmed temperature and the PM collected from the filter was quantified directly in the engine exhaust at different temperatures.

2. Experimental

2.1. Materials

The commercial fuels with sulfur contents of 6 ppm (S50) and 450 ppm (S500), which were used in the engine tests, were supplied by Petrobras and their main physicochemical properties are presented in Table 1. The tests were carried out using fuel doped with 5, 15, 25 and 50 ppm of ferrocene (Merck).

2.2. Sampling process

The tests were performed with a Toyama 7 Hp single cylinder engine, 250 cm^3, operating at 80% of maximum power, with

[a]*Instituto de Química, Universidade Federal do Rio Grande do Sul, Porto Alegre, RS, Av. Bento Gonçalves, 9500, 91501-970, Brasil. E-mail: rcv@ufrgs.br; Fax: +55 5133087304; Tel: +55 5133086306*
[b]*Engenharia Mecânica, Universidade Federal do Pampa, Alegrete, RS, Av. Tiarajú, 810, 97546-550, Brasil*

Table 1 Physicochemical properties of the fuel

	Specific gravity (kg m^{-3})	Viscosity (cSt)	90% Recovered (°C)	Flash point (°C)	Total sulfur (ppm)
Method	D4052	D445	D86	D93	D4294
S50	835	2.6	332	69	6
S500	850	3.3	354	68	450

mechanical injection; an average injection pressure of 150 bar, compression rate of 21 : 1, 3200 rpm, 10% of O_2 in the exhaust gases, and an average specific fuel consumption of 200 g/kW^{-1} h^{-1}. The soot was collected from the exhaust gas flow at an initial pressure differential of 300 mbar by means of a 47 mm diameter GF-1 Macherey-Nagel glass microfiber filter. The temperature of the filter element was adjusted using a furnace with electronically controlled temperature to ensure that the collected particulate matter was dry and contained the lowest possible amount of volatile hydrocarbons. A vacuum pump was used to impel the flow of gases through the filter element and, after cooling, the flow rate was determined using a Sensirion gas flow meter with a maximum nominal capacity of 20 mL min^{-1}.

2.3. Soot analysis

The catalytic soot oxidation activity generated in the tests was analyzed based on the reaction at the programmed temperature at a total flow rate of 20 mL min^{-1} of He with 2% of O_2, from room temperature to 900 °C, at a ramp rate of 10 °C min^{-1}, using a quartz reactor with 5 mg of PM and 50 mg of silicon carbide as a diluent. The reaction products – basically CO_2 – were analyzed with a Balzers mass spectrometer.

The soot particles collected from the combustion process were analyzed by transmission electron microscopy, using a JEOL 1200EX TEM microscope operating at 80 kV.

3. Results and discussion

The analysis of the results of this work focus on the effect of the quality of the fuel containing different concentrations of sulfur, and the effect of the presence of iron nanoparticles on the soot oxidation activity. The catalytic activity of the active sites formed by the thermal degradation of the ferrocene-doped fuel is analyzed in reactions at a programmed temperature and under real operating conditions in engine tests. The amount of retained particulate matter varies according to the temperature of the filter element and the quality of the fuel. Fig. 1 shows the mass of particulate matter retained as a function of the sampling temperature for the diesel with the highest sulfur content, S500, indicating that the mass of collected material increases as the sampling temperature decreases. At temperatures above 400 °C the mass of accumulated PM remains approximately constant, indicating that the condensation of unburned hydrocarbons is minimal in this temperature range, and that the oxidation speed is too low to detect a reduction in the accumulation of soot in the filter element. Higher amounts of PM accumulate are found at lower temperatures because, in fuel-rich regions inside the combustion chamber, the droplets of hydrocarbons with high molecular weight encounter greater difficulty in passing from the liquid to the vapor phase. During the injection of fuel, the hydrocarbon droplets in contact with heated air (N_2 + O_2) are

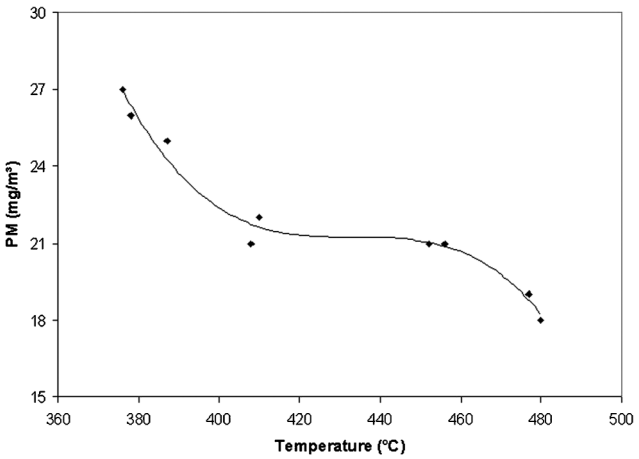

Fig. 1 Mass of PM retained (mg m^{-3}) as a function of sampling temperature using diesel S500 without the addition of ferrocene.

vaporized at their boiling point. The higher molecular mass fractions remain in the liquid phase, enabling the products of incomplete combustion to return to the liquid phase, which triggers a sequence of stages such as pyrolysis, nucleation, surface growth, coalescence and agglomeration.[15–23]

Fig. 2 illustrates the mass of particulate matter retained as a function of the sampling temperature for the S50 and S500 fuels doped with 50 ppm of ferrocene. These results indicate that the amount of retained PM from both fuels decreased significantly as the sampling temperature increased. The S50 diesel produced less soot than the S500 fuel, mainly due to the differences in their physicochemical properties, such as lower viscosity, final boiling point (T90) and specific gravity, which favor vaporization and combustion, generating lower amounts of particulate matter. The higher amount of PM collected from

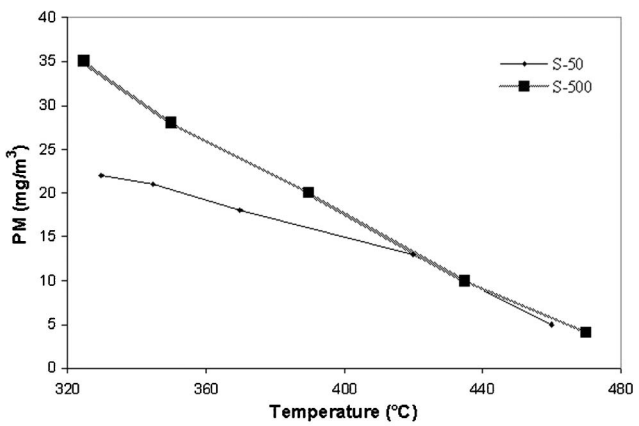

Fig. 2 Mass of PM retained as a function of sampling temperature from diesel with 50 ppm of ferrocene.

the S500 fuel at low temperatures is due to the higher amount of unburned hydrocarbons condensed on the soot surface.

Fig. 3 shows the mass of particulate matter as a function of the different amounts of ferrocene added to the fuel, for the S500 fuel, retained at an average sampling temperature of 460 °C, which is close to the average temperature of the exhaust gases. The S500 fuel with 50 ppm of ferrocene showed a reduction of approximately 80% in the amount of retained material (~4 mg m^{-3}) when compared with the diesel without the additive (~20 mg m^{-3}). Fuels doped with 50 ppm of ferrocene showed practically no accumulation of PM at sampling temperatures above 500 °C and the gas flow through the filter remained constant, indicating that the speed of oxidation was close to the speed of formation.

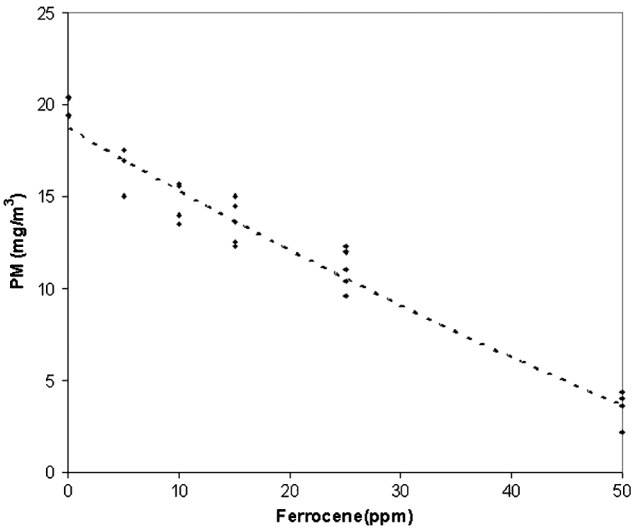

Fig. 3 Mass of retained soot particles (mg m^{-3}) as a function of the amount of ferrocene added to diesel S500 collected at an average temperature of 460 °C.

In the process of vaporization at temperatures between 400 and 500 °C and high pressures, the greater part of hydrocarbons, including ferrocene, is thermally degraded. The concentration of O_2 in the region around the droplet decreases due to hydrocarbon oxidation, and the concentration of H_2O and CO_2 increases. In a reducing atmosphere, the probability of the formation of reduced iron species (metallic Fe and F_3C) increases. Highly dispersed ultrafine FeOOH particles and crystalline structures of Fe_3O_4 are observed in the process of coal gasification.[24] In these conditions, the mechanism of soot oxidation should involve the following stages:

$$2Fe_3O_4\ (s) + 3H_2O\ (g) + 3C\ (s) \rightarrow 6FeOOH\ (s) + 3CO\ (g)$$

$$6FeOOH\ (s) + \tfrac{3}{2}O_2\ (g) \rightarrow 3H_2O\ (g) + 2Fe_3O_4\ (s)$$

The wide dispersal of the iron nanoparticles, which places the PM in close contact with the catalyst, leads to a sufficiently high oxidation rate to enable the filter element to self-regenerate. In addition, these results also demonstrate that fuels with sulfur content in the order of 500 ppm do not show significantly reduced catalytic activity in iron nanoparticle oxidation. The surface species formed by the condensation of sulfated compounds have a higher vapor pressure than the C and Fe species, favoring the condensation of compounds containing sulfur in the particle's outer region and diminishing the effect of the deactivation of active sites due to the formation of species containing SO_x.

Fig. 4 illustrates the gas flow through the filter element using an initial pressure differential of 300 mbar, as a function of sampling time, for the S500 fuel doped with different amounts of ferrocene. As can be seen, the gas flow rate remains at a higher level with increasing amounts of ferrocene, leading to a lower accumulation of PM. These results confirm that the presence of iron nanoparticles formed during combustion increases the catalytic activity of soot oxidation, reducing the restriction of the gas flow through the filter element.

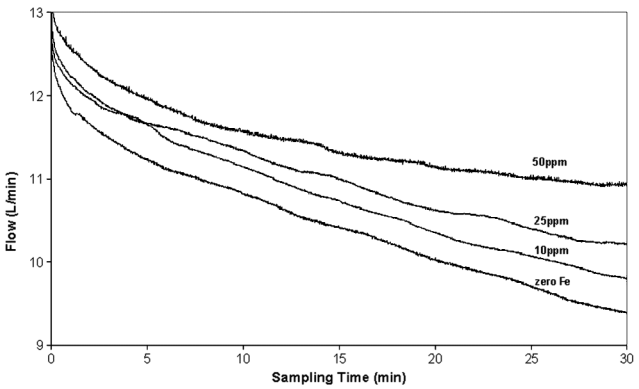

Fig. 4 Gas flow as a function of sampling time at a temperature of 460 °C for the S500 fuel.

Fig. 5 illustrates the catalytic activity of soot oxidation which was evaluated by means of reaction tests at a programmed temperature with oxygen for the S50 and S500 fuels. The highest peak in the profile of CO_2 evolution in both fuels, without the presence of ferrocene, was recorded at a temperature of 650 °C. The fuels doped with 50 ppm of ferrocene showed a shift of the highest CO_2 peak to lower temperatures of around 500 °C. These results indicate significantly increased oxidation activity in the presence of iron nanoparticles in close contact with the PM. They also confirm that the use of fuels doped with ferrocene allow for a soot oxidation speed analogous to that of its formation at the normal operating temperature of diesel engines, enabling the filter element to self-regenerate without the need to increase the temperature of the exhaust gases. The plausible mechanism involving the active sites formed by iron structures

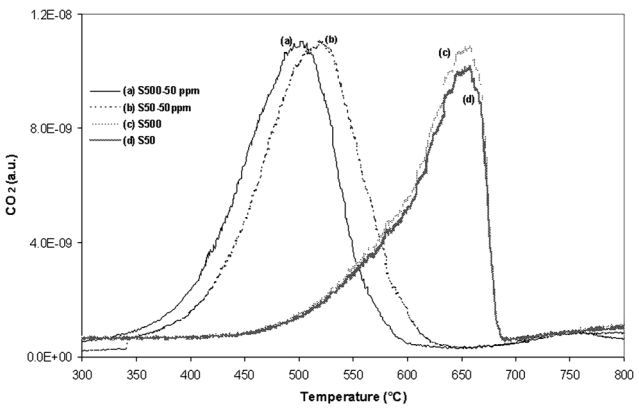

Fig. 5 Soot oxidation in reaction tests at a programmed temperature.

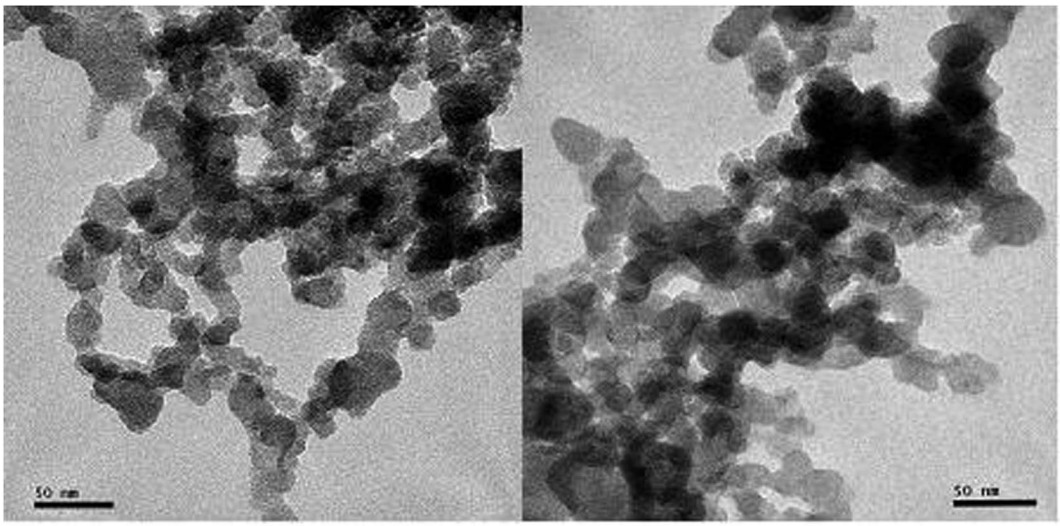

Fig. 6 TEM image of soot agglomerates from diesel doped with 50 ppm of ferrocene.

dispersed in the soot retained in the filter should involve the following stages: [24,25]

$$Fe_xO_y\ (s) + \tfrac{1}{2}O_2\ (g) \rightarrow Fe_xO_y\text{–}O\ (s)$$

$$Fe_xO_y\text{–}O\ (s) + C\ (s) \rightarrow Fe_xO_y\ (s) + CO\ (g)$$

Considering the mechanisms involve both reducing and oxidizing conditions, several solid-state species participate in the overall soot oxidation process, contributing for the overall speed to be controlled by diffusion phenomena of the active species. Thus, the soot should remain at a high temperature (500 °C) for a relatively long time to become completely oxidized.

Fig. 6 presents TEM images of soot agglomerates using diesel containing 50 ppm of ferrocene. Many of the particles resulting from the combustion process are agglomerates of organic matter with a high carbon content that are formed through the coagulation of elemental carbon spheres.[26–28] Iron nanoparticles have an average diameter of 10 nm and are distributed in the agglomerates. The dark regions shown in the TEM images correspond to structures with high Fe concentrations. The particulate matter retained in the filter, when using ferrocene-doped fuel, presents magnetic properties. Some regions show large agglomerates of spheres containing a high concentration of iron, indicating that the magnetic characteristics of the metallic Fe structures of Fe_3C contribute to subsequent coalescence. These particles are highly dispersed, thus presenting a close contact of the metal (catalyst) with the organic matter. The numerous active sites that act as catalysts in the oxidation process are responsible for the intense activity of these systems in the oxidation of particulate matter.

Conclusions

The catalytic activity of soot oxidation increases significantly in diesel fuels doped with 50 ppm of ferrocene, allowing for a reduction of up to 80% in emissions at the temperature of the exhaust gases under the normal operation of diesel engines. The onset of the soot oxidation reaction when using iron-doped diesel lies within the operating range of the diesel engine exhaust temperature, allowing for complete oxidation without the need to increase the temperature for the regeneration of the filter element. The formation of iron nanoparticles highly dispersed in the soot enables the close contact of the organic matter with the active sites, significantly increasing the catalytic activity of oxidation. In the operating conditions established in this work, regardless of the sulfur content and using 50 ppm of ferrocene in the fuel, the amount of PM accumulated in the filter was 0.02 g kW^{-1} h^{-1}.

Fuels doped with ferrocene lead to the formation of metallic iron nanoparticles in diesel engine exhaust emissions, thus representing new environmental implications. However, the use of exhaust gas particulate filters completely eliminates metal particle emissions into the environment, reducing the environmental impact caused by diesel engines.

Acknowledgements

The authors gratefully acknowledge the financial support of CAPES (Federal Agency for the Support and Evaluation of Postgraduate Education, Brazil).

References

1 E. W. de Menezes and R. Cataluña, *Quim. Nova*, 2008, **31**, 2027.
2 A. P. Sathiyagnanam and C. G. Saravanan, *Fuel*, 2008, **87**, 2281.
3 E. W. Menezes, R. Silva and R. Cataluña, *Fuel*, 2006, **85**, 815.
4 C. Y. Lin and K. H. Wang, *Fuel*, 2004, **83**, 507.
5 T. Kitamura, T. Ito, J. Senda and H. Fujiimoto, *JSAE Rev.*, 2001, **22**, 139.
6 H. Jung, D. B. Kittelson and M. R. Zachariah, *Combust. Flame*, 2005, **142**, 276.
7 G. A. Stratakis and A. M. Stamatelos, *Combust. Flame*, 2003, **132**, 157.
8 D. Uner, M. K. Demirkol and B. Dernaika, *Appl. Catal., B*, 2005, **61**, 334.
9 K. Villani, W. Vermandel and K. Smets, *Environ. Sci. Technol.*, 2006, **40**, 2727.

10 O. Ktocher, M. Elsener, A. Wokaun and K. Tikhomirov, *Appl. Catal., B*, 2006, **64**, 72.
11 I. Atribak, B. Azambre, A. Bueno López and A. García-García, *Appl. Catal., B*, 2009, **92**, 126.
12 K. Irani, W. S. Epling and R. Blint, *Appl. Catal., B*, 2009, **92**, 422.
13 B. Kegl, *Energy Fuels*, 2007, **21**, 3310.
14 J. Beckers and G. Rothenberg, *ChemPhysChem*, 2005, **6**, 223.
15 J. P. A. Neeft, M. Makkee and J. A. Moulijn, *Fuel Process Technol*, 1996, **1**, 47.
16 J. C. Guibet, E. Faure-Birchem, in *Fuels and Engines*, Paris: Technip 2, 1999, pp. 786.
17 B. Harrison, M. Wyatt and G. Gough, *Catalysis*, 1982, **5**, 127.
18 J. M. D. Cónsul, D. Thiele, R. Cataluña and I. M. Baibich, *Quim. Nova*, 2004, **27**, 432.
19 P. Zelenka, W. Cartellieri and P. Herzog, *Appl. Catal., B*, 1996, **10**, 3.
20 M. M. Maricq, *J. Aerosol Sci.*, 2007, **38**, 1079.
21 D. B. Kittelson, *J. Aerosol Sci.*, 1998, **29**, 575.
22 SAE, 1993. In: 1993 SAE Hanbook, v. 3, in *Engines, Fuels, Lubrificants, Emissions, and Noise Society of Automotive Engineers*, Warrendale, PA, 25.
23 D. R. Tree and K. I. Svensson, *Prog. Energy Combust. Sci.*, 2007, **33**, 272.
24 H. Yamashita, S. Yoshida and A. Tomita, *Energy Fuels*, 1991, **5**, 52.
25 K. Zhai, H. Wang and Y. G. Wei, *J. Phys. Chem. C*, 2009, **113**, 15288.
26 R. E. Franklin, *Acta Crystallogr.*, 1951, **4**, 253.
27 A. Braun, N. Shah and F. E. Huggins et.al, *Carbon*, 2005, **43**, 2588.
28 A. Braun, F. E. Huggins and K. E. Kelly et.al, *Carbon*, 2006, **44**, 2904.

